PHYSICAL REVIEW B VOLUME 26, NUMBER 12 15 DECEMBER 1982

Atomic structure of amorphous particles produced by spark erosion

S. Aur and T. Egami
Department of Materials Science and Engineering and Laboratory for Research on the Structure of Matter, University of Pennsylvania, Philadelphia, Pennsylvania 19104

A. E. Berkowitz and J. L. Walter
General Electric Corporate Research and Development, Schenectady, New York 12301
(Received 13 August 1982)

The atomic structure of amorphous particles of composition $Fe_{75}Si_{15}B_{10}$ produced by spark erosion was studied by the energy-dispersive x-ray diffraction technique and was compared to that of the amorphous ribbon of the same composition produced by melt spinning. It was found that the nearest-neighbor Fe-Fe correlation is almost identical for the ribbon and the particles of different sizes, whereas the second peak of the radial distribution function shows considerable differences among the samples. The result is consistent with decreased metal-metalloid compositional short-range order in the particles compared to that in the ribbon sample.

I. INTRODUCTION

Metallic amorphous alloys can be produced by various methods, all of which involve a rapid cooling on either a macroscopic or microscopic scale, to avoid nucleation and growth of crystals.[1–3] The physical properties of the alloys generally depend on the method and conditions of production.[4–6] However, most of the variations observed among the alloys produced by more commonly employed methods, such as melt spinning, sputtering, and electrodeposition, appear to be the consequences of different degrees of structural relaxation[7–9] and macroscopic structural or compositional inhomogeneity.[10] The direct comparison of the structure of the alloys produced by different methods is difficult and rare, but the available data indicate that the atomic structure is basically the same for the alloys produced by melt spinning, electrodeposition, and sputtering within the variations expected for different degrees of structural relaxation.[11]

Recent studies showed, however, that amorphous particles produced by spark erosion[12] exhibit markedly different properties, indicating that there may be some fundamental structural differences between the amorphous alloys produced by spark erosion and those produced by other methods.[13,14] It was found that the particles have smaller magnetization and Curie temperature compared to amorphous ribbons of the same composition produced by melt spinning. Furthermore, the hyperfine field distribution of the particles was observed to be broader and its average value smaller as compared to the ribbon, suggesting that the particles have less local compositional short-range order (CSRO). The differences in the properties depend also on the particle size. Smaller particles showed more deviations from the ribbons than did large particles. It was suggested, therefore, that the faster quench rate of spark erosion as compared to melt spinning, particularly for small particles, produced the decrease in CSRO.[13,14] Since the direct measurement of CSRO is a difficult task, we have examined the total x-ray radial distribution function (RDF) by the energy-dispersive x-ray diffraction (EDXD or XRED) method.[15–17] It was found that the RDF shows significant differences which are much larger than expected for different degrees of structural relaxation. These differences are consistent with the decreased CSRO in the amorphous particles produced by spark erosion compared with the ribbon.

II. EXPERIMENTAL

Amorphous particles of the composition $Fe_{75}Si_{15}B_{10}$ were produced by spark erosion in dodecane $[CH_3(CH_2)_{10}CH_3]$.[13] The particles are identical to the ones used for previous studies, with the size ranging from 0.5 to 30 μm in diameter.[14] Details of the methods are described in Ref. 14. Chemical analysis[12,13] showed that the particles have no carbon contamination which could have resulted from the decomposition of the dielectric fluid. Mössbauer analysis and electron microscopy of crystallized samples were consistent with the

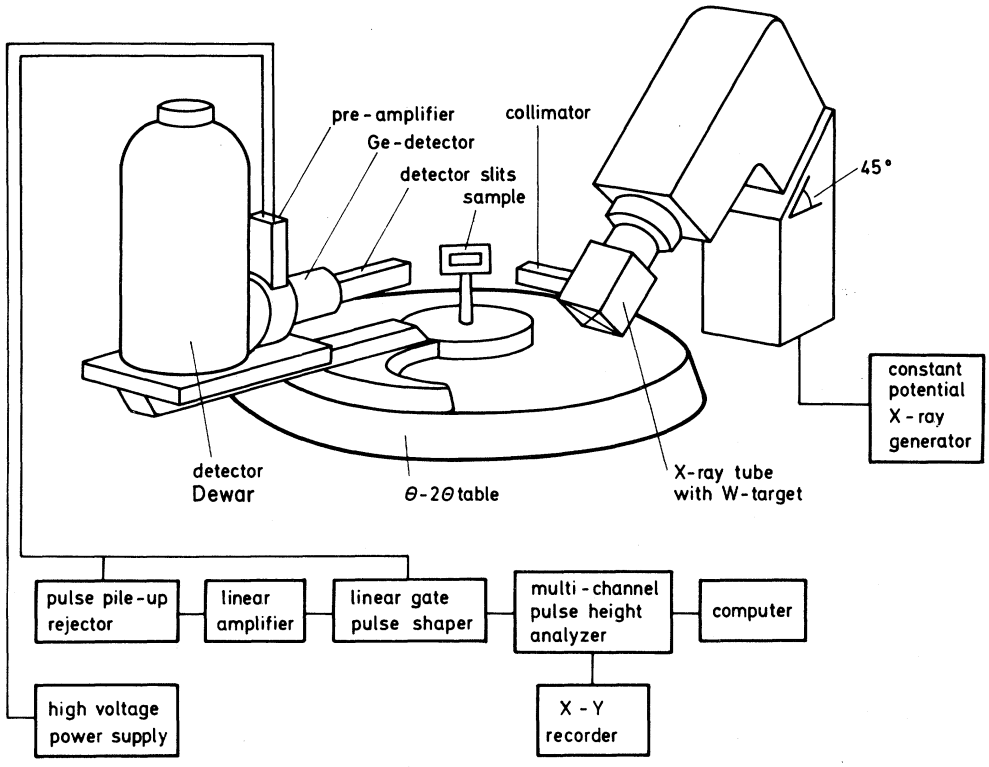

FIG. 1. Energy-dispersive x-ray diffraction apparatus used for the present study (Ref. 16).

composition of the starting material. Therefore, it appears that the chemical composition of the particles is essentially the same as that of the starting material, and that the observed differences in magnetic properties are not caused by composition variations.

In the EDXD (or XRED) method, the structural information is obtained through x-ray spectroscopy of the diffracted white x-ray beam, using an intrinsic Ge photon detector. Because of the high intensity of the white x rays, in this case from a W target tube, the method provides a very accurate determination of the structure factor. Furthermore, it permits probing a much wider q space than does the conventional method. In this study, the structure factor $i(q)=S(q)-1$ was determined up to 25 Å^{-1}. This totally eliminates the termination error,[18] so that the Fourier transform to obtain the RDF from $i(q)$ can be carried out without any artificial treatments. The apparatus shown in Fig. 1 consists of an x-ray tube tilted 45° in order to eliminate the effect of polarization, an intrinsic Ge detector with a resolution of 155 eV at 6.9 keV and 230 eV at 40 keV, a pulse pileup rejector, a multichannel pulse height analyzer with 1024 channels, and a PDP 11/10 minicomputer. The diffraction experiment was carried out in reflection geometry at the diffraction angles $\theta=5°$, 7.5°, 10°, 15°, 20°, 30°, and 40°. The x-ray spectra were corrected for air scattering, escape peaks, multiple scattering, and inelastic Compton scattering, and were combined to yield the interference function $i(q)$.[16]

III. RESULTS

The amorphous particles produced by spark erosion were sorted into three size fractions, 0.5–5, 10–20, and 20–30 μm. The interference function $i(q)$ for these three size fractions of particles and the amorphous ribbons of the same composition obtained by melt spinning are shown in Figs. 2 and 3. Significant differences are observed in the first peak and in the shoulder of the second peak. The first-peak and second-peak shoulder of the ribbon sample are considerably higher than those of the particles, indicating a greater degree of short-range order in the ribbon sample. The height of the second-peak shoulder follows the trend of the particle size; the smaller the particles, the lower the shoulder. The

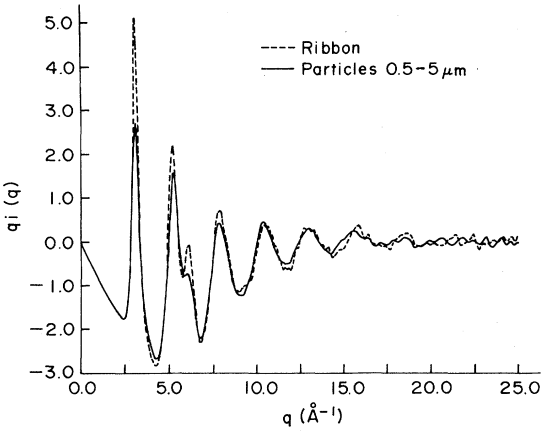

FIG. 2. Structure factor $qi(q)$ of amorphous ribbons of $Fe_{75}Si_{15}B_{10}$ and particles with 0.5—5 μm in diameter.

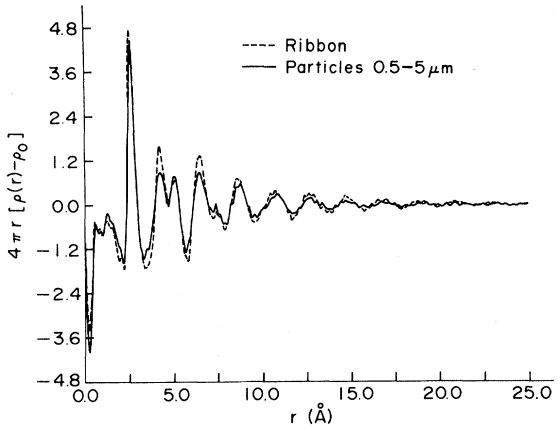

FIG. 4. RDF's $4\pi r[\rho(r)-\rho_0]$ of amorphous $Fe_{75}Si_{15}B_{10}$ obtained by melt spinning in ribbon form and obtained by spark erosion in the form of particles.

RDF's obtained by the direct Fourier transform of the $i(q)$'s for these samples,

$$G(r)=4\pi r[\rho(r)-\rho_0]=\frac{2}{\pi}\int i(q)\sin(qr)q\,dq\ , \tag{1}$$

are shown in Figs. 4—6. It is immediately noticed that the heights and positions of the first-peak and second-peak shoulder at about 5 Å are virtually identical for all samples, while the second and third peaks show significant differences. Furthermore, the ribbon sample shows a distinct prepeak of the first peak at about 2 Å, while the prepeaks of the particles are smeared. These results suggest that the nearest-neighbor Fe-Fe correlation (first peak) and the Fe-Fe-Fe collinear correlation (second-peak shoulder) are similar in all samples; however, the Fe-Fe correlations involving metalloids in between appear to be dependent on the preparation as discussed below.

It is generally difficult to compare the structure of samples with different geometry, since the absorption of x ray depends upon the details of the sample geometry. However, the differences in $i(q)$ and $G(r)$ observed here are definitely beyond the uncertainty due to such an effect. For instance, the

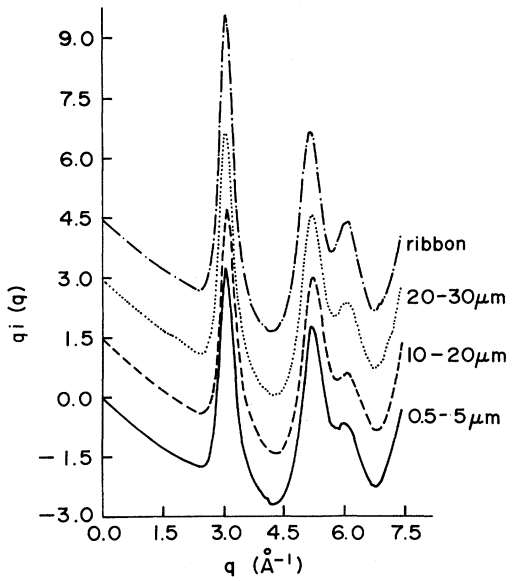

FIG. 3. Structure factor $qi(q)$ of ribbons of $Fe_{75}Si_{15}B_{10}$ and particles with various sizes.

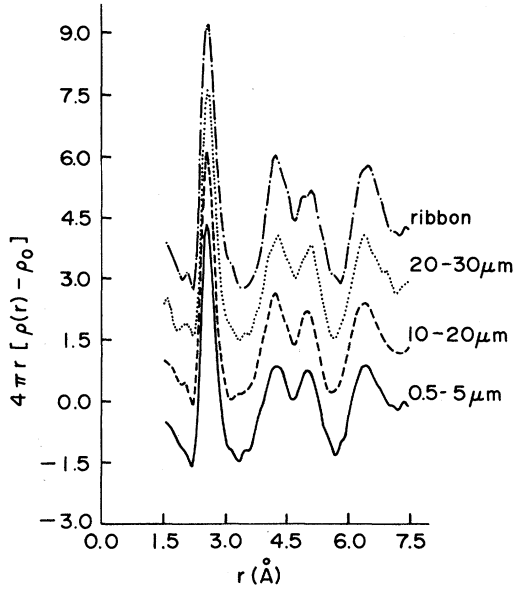

FIG. 5. RDF of $Fe_{75}Si_{15}B_{10}$ ribbons and those of $Fe_{75}Si_{15}B_{10}$ in various particle sizes.

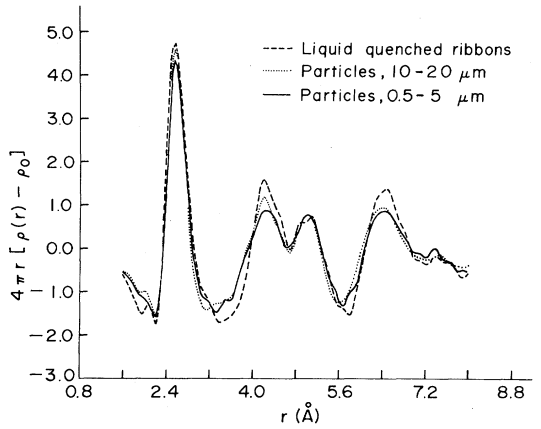

FIG. 6. RDF's of $Fe_{75}Si_{15}B_{10}$ obtained by melt spinning (ribbons) and by spark erosion (particles).

clear difference in the amplitude of $i(q)$ shown in Figs. 2 and 3 cannot result from the absorption effect alone. Since the differences in the heights of the second and third peaks of $G(r)$ are primarily the consequences of the differences in the first peak of $i(q)$, we are convinced that these differences are real. On the other hand, the differences in the prepeak at 2 Å are less convincing, since its amplitude is similar to amplitudes of spurious peaks which are seen below 1.8 Å. The origin of these spurious peaks is not known, but it is presumably the combination of the inaccuracies in the absorption correction and inelastic scattering correction. Such spurious oscillations appear in most RDF determinations.

IV. DISCUSSION

As shown in Figs. 4–6, a conspicuous difference between the RDF of the ribbon sample and those of the particles was found in the second-peak height. Unlike the first-peak and second-peak shoulder, the second peak is affected by the details of the topology, and in the case of alloys, by the sizes of the constituent atoms and the CSRO. Therefore, it is intuitively understood that the reduced height of the second peak of the particles obtained by spark erosion indicates the reduced CSRO in the particles compared to the melt-spun ribbons, which is consistent with the conclusion in Ref. 13. In order to discuss this point further, we will review our present state of understanding about CSRO, and compare the present results to the case of amorphous Fe_3B and Ni_2FeB, in which a similar difference in the second peak was found.[19,20]

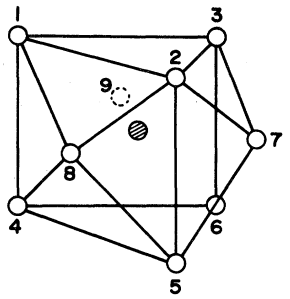

FIG. 7. Capped trigonal prism of transition-metal atoms around a metalloid atom.

It is widely recognized that although the dense random packing (DRP) model provides a good description of monoatomic liquids and a convenient starting point to model the structure of polyatomic glasses,[21] the actual short-range order in polyatomic glasses is often not as random as the DRP model suggests.[22] It has been proposed that the RDF and the hyperfine field distribution of metal-metalloid glasses are better explained if we assume a short-range order similar to the one found in the corresponding crystalline compounds.[19,22–24] In particular, Gaskell[23] suggested that the structure may be composed of capped trigonal prisms of transition-metal atoms, with a metalloid atom at the center of each prism (Fig. 7). Such trigonal prisms are commonly found in the transition-metal–metalloid compounds with complex structures such as the orthorhombic Fe_3C structure (DO_{11}, isomorphous to Pd_3Si, Pd_3B, Ni_3B, etc.) and the tetragonal Fe_3P structure (DO_e) and its derivative Fe_3B.[25] As pointed out by Aronsson and Rundqvist,[26] the formation of such a structure is, in fact, a very natural consequence of the local close packing. If one attempts to pack B atoms around an A atom to form a close-packed cluster of atoms, the number of B atoms which can be the nearest neighbor of the A atom, N_{AB}, depends upon the ratio of the radii of A and B atoms. If $r_A = r_B$, N_{AB} is between 12 and 13. If $r_A/r_B = 0.902$, $N_{AB} = 12$, and the cluster is an icosahedron. The capped trigonal prism ($N_{AB} = 9$) is formed when $r_A/r_B = 0.732$ ($= \sqrt{3} - 1$). In other words, the inscribed radius of the Bernal hole of the capped trigonal prism is 0.732, when the radius of the peripheral atoms is unity. Fe and P satisfy this condition fairly well, with $r_P/r_{Fe} = 0.75$ (in Fe_3P), so that a P atom in Fe_3P is at the center of an almost ideal capped trigonal prism of Fe atoms.[27] Therefore, as long as P atoms are surrounded only by Fe atoms, that is, P atoms are not nearest neighbors, the capped trigonal prisms are expected to be found even in the random close-packed structure.

The DRP model of Fe-P produced by Fujiwara and Ishii[28] demonstrates that this is indeed the case. They took the size ratio to be $r_P/r_{Fe}=0.72$, and constructed the DRP model in such a way to avoid the nearest-neighbor presence of P atoms around P atoms. They found that about 50% of P atoms are at the center of the capped trigonal prisms.

The structure of Fe_3B has been reported to be either tetragonal[29,30] or orthorhombic,[30,31] and no single-crystal study has been made. Judging from the study of the Fe_3 (P,B) system,[25] the structure of Fe_3B must be body-centered tetragonal (ϵ_1 phase), with the lattice constants $a=8.62$ Å and $c=4.31$ Å, which is consistent with the electron-microscopy study.[32] The ϵ_1 phase was found for $Fe_3P_{1-x}B_x$ ($0.4<x<0.94$), and a single-crystal study was done for $x=0.63$.[25] The structure of the ϵ_1 phase is closely related to that of the $\epsilon-Fe_3P$, with the metalloid atom also located at the center of a capped trigonal prism of Fe atoms. With the use of the lattice constants extrapolated to Fe_3B, as above, and the atomic position parameters determined for $Fe_3P_{0.37}B_{0.63}$, the lattice structure of Fe_3P can be reasonably assumed. We then calculated the average Fe-Fe and Fe-B nearest-neighbor distances $\bar{r}_{Fe\text{-}Fe}$ and $\bar{r}_{Fe\text{-}B}$, since the structure is complex and the atomic distances are distributed. The atomic radii of Fe and B were then calculated, assuming $r_{Fe}=\bar{r}_{Fe\text{-}Fe}/2$ and $r_B=\bar{r}_{Fe\text{-}B}-r_{Fe}$. They are $r_{Fe}=1.30$ Å, $r_B=0.91$ Å, and $r_B/r_{Fe}=0.70$. This size ratio indicates that B atoms are located in nearly ideal capped trigonal prisms, and in fact $r_{Fe\text{-}B}$ has a relatively narrow distribution (2.13–2.28 Å). On the other hand,[33] in Ni_3B the B-Ni distance (2.04 Å) is appreciably smaller than the B-Fe distance (2.21 Å) due to the stronger interaction between B and Ni.[26,34] Thus the boron radius appears to be smaller, with $r_B=0.78$, while $r_{Ni}=1.26$, so that $r_B/r_{Ni}=0.62$. In this case the trigonal prism become crushed, with the capping atoms extended further out. In fact, it is closer to the trigonal prism *without* caps, of which inscribed radius is 0.528 ($=\sqrt{7/3}-1$). In addition the crystal structure is no longer the tetragonal structure, but becomes the orthorhombic (cementite) structure. An important difference between these two cases is that in Fe_3B the distance between the capping atom and the atom in the opposite corner of the trigonal prism (R_{17} in Fig. 7) is similar to the diagonal distances within the prism, such as R_{15} and R_{16}, but it is larger in Ni_3B. This difference is reflected in the RDF of Fe_3B and Ni_2FeB shown in Fig. 8 as the height of the second peak at 4.0 Å; the second peak of Fe_3B is higher than that of Ni_2FeB. The same result is obtained in the quasicrystal model shown in Fig. 9 which was obtained by simply broadening the RDF of crystals by a Gaussian distribution which represents random strain with the mean amplitude of 5%.[19]

The effect of Si substitution for B on the crystal structure is not well documented in the literature except that the formation of DO_{11} cementite structure was reported for Fe_3 (B,Si).[35] The examination of the structure of[36] Ni_6Si_2B which is isotypic to

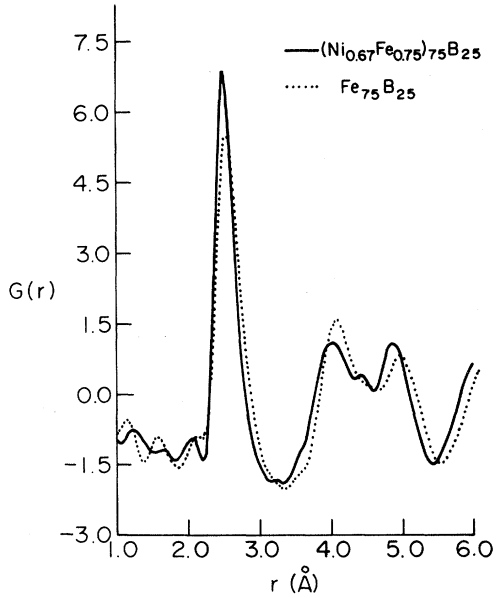

FIG. 8. RDF's of amorphous $Fe_{75}B_{25}$ and amorphous $Fe_{25}Ni_{50}B_{25}$ (Ref. 19).

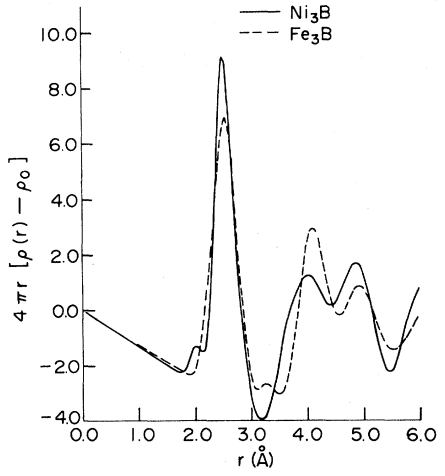

FIG. 9. RDF's of crystalline Fe_3B and $FeNi_2B$ broadened by a Gaussian distribution to simulate the randomness.

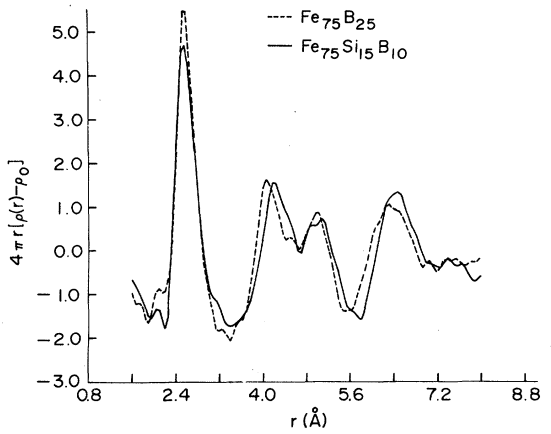

FIG. 10. RDF's of amorphous $Fe_{75}Si_{15}B_{10}$ and $Fe_{75}B_{25}$ ribbons.

Fe_2P, and those of[35] $Fe_{4.86}Si_2B$ and $Co_{4.7}Si_2B$, indicates that Si atoms also basically occupy the center of the capped trigonal prism, with possible substitution to Fe site. Therefore, it is reasonable to assume that even in the liquid state, Si atoms tend to avoid either Si or B atoms as nearest neighbors if the temperature is not high enough to destroy the local CSRO. In fact, the RDF's of $Fe_{75}B_{25}$ and $Fe_{75}Si_{15}B_{10}$ ribbons are quite similar, as shown in Fig. 10. The second peak of the RDF of $Fe_{75}Si_{15}B_{10}$ ribbon is as sharp as that of $Fe_{75}B_{25}$, indicating a high degree of local order around the metalloid atoms, although it is shifted to larger values of r, reflecting the slight difference in the size between Si and B atoms ($r_{Si} \sim 1.10$ Å). However, if the local CSRO is reduced, the trigonal prisms will be distorted since both the coordination number and composition around Si and B atoms will be different from nine Fe atoms which make up the capped trigonal prism. Then the second peak of RDF will become lower, and Fe-(B,Si) peak (subpeak at around 2.1 Å) will become smeared. Fe-Fe and collinear Fe-Fe-Fe correlations remain largely unchanged, so that the first-peak and second-peak shoulder of RDF would remain the same. These predictions are consistent with observations shown in Figs. 5—7. Furthermore, recent studies of crystallization of an $Fe_{75}Si_{15}B_{10}$ ribbon and $Fe_{75}Si_{15}B_{10}$ particles have shown that the first crystals to nucleate and grow have dissimilar crystal structures in the two materials.[37] This result corroborates the above results and will be discussed in another paper.

If the CSRO in the particles is more random than in the ribbon, then it may appear to be difficult to understand why annealing treatment apparently did not change it,[13] while in other systems, such as Fe-Ni base alloys, annealing is considered to change the CSRO.[38,39] It should be noted, however, that in the latter case the change in the CSRO occurs presumably among the transition-metal atoms, while in the present case we are presuming the change in the CSRO between transition metals and metalloids, which would be more difficult because of the differences in size and electronic structure. Furthermore, the differences in the RDF found here are much larger than those observed during the structural relaxation.[17] Therefore, it is likely that the process to change such a CSRO would involve higher activation energies, and may not be achieved in the glassy state.

V. CONCLUSION

The total x-ray radial distribution functions of amorphous $Fe_{75}Si_{15}B_{10}$ particles produced by spark-erosion technique were determined by the energy-dispersive x-ray diffraction, and were compared to that of amorphous ribbons obtained by melt spinning. Since the compositional partial RDF's have not been resolved, we do not have a direct knowledge of the CSRO. Nevertheless, the result shows distinct differences in the RDF between the particles and the ribbon, which are consistent with the reduced local CSRO around the metalloid atoms in the amorphous particles produced by spark erosion. Such a reduced CSRO could result from the high rate of cooling and the high liquid temperature prior to quenching that are achieved during the spark-erosion process, and are consistent with other physical properties previously studied.

ACKNOWLEDGMENTS

The authors gratefully acknowledge Dr. G. S. Cargill III and Dr. H. S. Chen for helpful comments on the atomic-size effects. A part of this work at the University of Pennsylvania was supported by the NSF via the Materials Research Laboratory (MRL) Grant No. DMR79-23647.

[1]P. Duwez, Ann. Rev. Mat. Sci. 6, 83 (1976).
[2]H. A. Davies, in *Rapidly Quenched Metals III,* edited by B. Cantor (The Metals Society, London, 1978), Vol. 1, p. 1.
[3]H. S. Chen, H. J. Leamy, and C. E. Miller, Ann. Rev. Mat. Sci. 10, 363 (1980).
[4]G. C. Chi, H. S. Chen, and C. E. Miller, J. Appl. Phys. 49, 1715 (1978).
[5]T. Takayama and T. Oi, J. Appl. Phys. 50, 1595 (1979).
[6]F. E. Luborsky and H. H. Liebermann, Mater. Sci. Eng. 49, 257 (1981).
[7]G. Dietz and K. Hüller, J. Non-Cryst. Solids 47, 377 (1982).
[8]T. Egami and S. D. Dahlgren, J. Appl. Phys. 49, 1703 (1978).
[9]Y. Waseda and T. Egami, J. Mater. Sci. 14, 1249 (1979).
[10]G. C. Chi and G. S. Cargill III, in *Magnetism and Magnetic Materials—1975 (Philadelphia),* Proceedings of the 21st Annual Conference on Magnetism and Magnetic Materials, edited by J. J. Becker, G. H. Lander, and J. J. Rhyne (AIP, New York, 1976), p. 147.
[11]K. Suzuki, F. Itoh, T. Fukunaga, and T. Honda, in *Rapidly Quenched Metals III,* edited by B. Cantor (The Metals Society, London, 1978), Vol. 2, p. 410.
[12]T. Yamaguchi and K. Narita, IEEE Trans. Mag. MAG-13, 1621 (1977).
[13]A. E. Berkowitz, J. L. Walter, and K. F. Wall, Phys. Rev. Lett. 46, 1484 (1981).
[14]A. E. Berkowitz and J. L. Walter, Mater. Sci. Eng. 55, 275 (1982).
[15]M. Mantler and W. Parrish, in *Advances in X-ray Analysis* (Plenum, New York, 1976), Vol. 20, p. 171.
[16]T. Egami, in *Glassy Metals I,* edited by H.-J. Güntherodt and H. Beck (Springer, Berlin, 1981), p. 25.
[17]T. Egami, J. Mater. Sci. 13, 2587 (1978).
[18]S. Aur and T. Egami, J. Phys. (Paris) 41, C8-234 (1980).
[19]S. Aur and T. Egami, in *Proceedings of the International Conference on Rapidly Quenched Metals, IV,* edited by T. Masumoto and K. Suzuki (The Japan Institute of Metals, Sendai, 1982), Vol. 1, p. 351.
[20]S. Aur, thesis, University of Pennsylvania, 1981 (unpublished).
[21]G. S. Cargill III, Solid State Phys. 30, 227 (1975).
[22]P. H. Gaskell, J. Phys. C 12, 4337 (1979).
[23]P. H. Gaskell, J. Non-Cryst. Solids 32, 207 (1979).
[24]I. Vincze, D. S. Boudreaux, and M. Tegze, Phys. Rev. B 19, 4896 (1979).
[25]S. Rundqvist, Acta Chem. Scand. 16, 1 (1962).
[26]B. Aronsson and S. Rundqvist, Acta Crystallogr. 15, 878 (1962).
[27]S. Rundqvist, Ark. Kemi. 20, 67 (1962).
[28]T. Fujiwara and Y. Ishii, J. Phys. F 10, 1901 (1980).
[29]J. L. Walter, S. F. Bartram, and R. R. Russell, Metall. Trans. 9A, 803 (1978).
[30]U. Herold and U. Koster, Z. Metallkde. 69, 326 (1978).
[31]R. Hasegawa, R. C. O'Handley, and L. I. Mendelsohn, in *Magnetism and Magnetic Materials—1976 (Joint MMM-Intermag Conference, Pittsburgh),* Partial Proceedings of the first joint MMM-Intermag Conference, edited by J. J. Becker and G. H. Lander (A.I.P., New York, 1976), p. 298.
[32]J. L. Walter, S. F. Bartram, and I. Mella, Mater. Sci. Eng. 36, 193 (1978).
[33]S. Rundqvist, Acta Chem. Scand. 12, 658 (1958).
[34]R. P. Messmer, Phys. Rev. B 23, 1616 (1981).
[35]B. Aronsson and G. Lundgren, Acta Chem. Scand. 13, 433 (1959).
[36]S. Rundqvist and F. Jellinek, Acta Chem. Scand. 13, 425 (1959).
[37]J. L. Walter, A. E. Berkowitz, and E. F. Koch (unpublished).
[38]T. Egami, Mater. Res. Bull. 13, 557 (1978).
[39]T. Egami, IEEE Trans. Mag. MAG-17, 2600 (1981).